Lawrence Berkeley National Laboratory

Lawrence Berkeley National Laboratory

Title

Local indium segregation and band structure in high efficiency green light emitting InGaN/GaN diodes

Permalink

https://escholarship.org/uc/item/5ts1r9gq

Authors

Jinschek, Joerg R.
Erni, Rolf
Gardner, Nathan F.
et al.

Publication Date

2004-11-23

NATURE MATERIALS LETTER:

Local Indium Segregation and Band Structure in High Efficiency Green Light Emitting InGaN/GaN Diodes.

Joerg R. Jinschek [1], Rolf Erni [2], Nathan F. Gardner [3], Andrew Y. Kim [3], and Christian Kisielowski [1]

[1] National Center for Electron Microscopy (NCEM), Ernest Orlando Lawrence Berkeley National Laboratory (LBNL), 1 Cyclotron Road MS 72R0150, Berkeley/California 94720, U.S.A.

[2] Department of Chemical Engineering and Materials Science, University of California Davis, Davis/California 95616, U.S.A.

[3] Lumileds Lighting, San Jose/California 95131, U.S.A.

Correspondence requests for materials should be addressed to C.K.

(e-mail: CFKisielowski@lbl.gov)

Date of submission: 23. Nov. 2004

GaN/InGaN light emitting diodes (LEDs) are commercialized for lighting applications because of the cost efficient way that they produce light of high brightness[1,2]. Nevertheless, there is significant room for improving their external emission efficiency[3] from typical values below 10%[4] to more than 50%[5], which are obtainable by use of other materials systems that, however, do not cover the visible spectrum. In particular, green-light emitting diodes fall short in this respect[1-3], which is troublesome since the human eye is most sensitive in this spectral range. In this letter advanced electron microscopy is used to characterize indium segregation in InGaN quantum wells of high-brightness, green LEDs (with external quantum efficiency as high as 15% at 75 A/cm^2). Our investigations reveal the presence of 1-3 nm wide indium rich clusters in these devices with indium concentrations as large as 0.30-0.40 that narrow the band gap locally to energies as small as 2.65 eV.

The electronically active region of green LEDs typically consists of stacked, few nm wide $In_XGa_{1-X}N$ ($x \sim 0.2$) quantum wells that are sandwiched between p- and n-doped GaN. The photon emission energy and external device efficiency depend on the device architecture, the fraction x of In atoms substituting Ga sites in the quantum wells, the quantum well width, and the homogeneity of the indium distribution in the well[1,2,6,7]. Parameters such as well width, device architecture, or the average In content can be optimized relatively well to enhance efficiencies for a particular emission wavelength. The homogeneity of the indium distribution, on the other hand, is widely debated[6,7] and it was argued that a miscibility gap limits the In solubility in GaN[8] leading to local segregation and the formation of “dot-like” structures within quantum wells[6,7]. In fact, it is uncertain how device efficiencies are affected by a particular indium distribution.

This uncertainty arises from the limited experimental ability to map the indium concentration at atomic resolution and to link this information to the electronic structure in devices. Electron microscopy is a most suitable tool for this purpose and addressed this issue with some success in the past[9,10]. In this letter, we utilize advanced microscopy techniques to investigate the indium distribution in commercially available devices. We demonstrate for the first time that an unusually high external quantum efficiency of 15% at a drive current density of 75 A/cm^2 can be obtained from samples that exhibit a quantified amount of local indium segregation and band gap variation.

Electron transparent samples were prepared site specific from these devices by a focused ion beam method. It is essential to control preparation and radiation induced damage in such experiments[11] that we addressed by optimizing the sample preparation process and by minimizing exposure to the electron beam[12]. Figure 1 shows dark-field electron micrographs of the active LED region in the $[11\underline{2}0]$ zone axis orientation at medium and high resolution. The contrast difference between indium (Z=49) and gallium (Z=31) is generated by an atomic number Z contrast[13,14] and indium-rich clusters in the quantum wells with sizes in the range of 1-3 nm are seen. The presence of such "quantum dot-like" structure was discussed before[7,15,16] but rarely linked to commercial device performance and never quantified in terms of absolute local indium concentration together with band gap variation.

A visualization of these clusters by Z-contrast imaging is suitable[9,17]. However, a quantification of the indium concentration from Z-contrast images is currently hardly possible[10]. Therefore, we utilize lattice images recorded in a high voltage electron microscope to determine absolute local In concentration in the quantum wells. The applied method maps the local indium concentration by extracting local distortion of single unit cells (0.5 x 0.3 nm^2) that directly relate to the substitution of the gallium atoms by the larger indium atoms. These extractable distortions were calibrated to provide absolute values for local indium concentrations[18].

The Figure 2 shows both, a displacement map as well as an averaged profile. The average expansion of the c lattice parameter inside the quantum well reaches 4% and relates to an indium fraction $x = 0.17 \pm 0.01$ in good agreement with the nominal In concentration of $x = 0.20$. Green light is emitted at a wavelength of about 530 nm from this well with 3.5 ± 0.5 nm of average width. The lower interface is seen to be more abrupt than the upper one, which reflects the growth direction that points from bottom to top in this picture. The effect has been reported before[17,19]. Furthermore, the indium map in Fig. 2c reveals significant local unit cell size fluctuations reaching 8% that corresponds to a local indium fraction x of 0.30 - 0.40. A diameter of 1-3 nm of these indium-rich domains compares well with the dark-field observation and it is seen that local indium enrichment is accompanied by indium depletion from the surrounding area.

Structural and compositional information extracted from the electron micrographs can be combined with spatially resolved band gap information by applying high energy-resolution valence electron energy loss spectroscopy (VEELS)[20-22]. In our experiments, a beam size of ~ 1nm was combined with an energy resolution of better than 200 meV that allows probing the InGaN band gap locally.

Figure 3a shows two VEEL spectra taken from the GaN barrier (solid line) and inside the InGaN quantum well (open circles). The intensity onsets around 3 eV correspond to the band gap signals. Plasmon excitation peaks at 19.2 ± 0.1 eV for GaN and 18.6 ± 0.1 eV for InGaN agree with previous studies[23]. The position of the plasmon peak in the InGaN QW can be related to an In content x between 0.15 and 0.20[23], which matches with our estimated averaged In content derived from HRTEM (x ~0.17).

In Fig. 3b three low-loss spectra from different GaN barrier regions confirm the reproducibility and reliability of the local VEELS measurements since the observed variations are marginal (< 0.02 eV). Fig. 3c identifies the direct band gap of hexagonal GaN with an energy E_g of 3.30 ± 0.10 eV by fitting an expected power law $(E-E_g)^{0.5}$ (dashed line) to the data[20-22]. The result agrees with literature data 3.3 eV[24] and 3.35 eV[25]. Stepping the electron probe along the centre of the quantum wells and measuring low-loss spectra reveal a variation of the band gap energy Eg inside the quantum wells. Two examples are shown in Fig. 3d and 3e, which illustrate band gap variations along the length of the quantum wells. For example, we find dominant band gap energies of 2.90 eV and 3.15 eV, respectively, in these cases. Moreover, a less dominant transition at 2.65 eV is superimposed. Considering the $In_XGa_{1-X}N$ band gap bowing parameter from data of bulk materials[26], the 2.90 eV and 3.15 eV onsets correspond to an In content x of 0.25 and 0.14, respectively. The second, less intense onset at E_g=2.65eV suggests the simultaneous presence of clusters with an indium concentration as large as $x \sim 0.38$.

All extracted local $In_XGa_{1-X}N$ band gap data are plotted in Figure 4 and compared with a Poisson distribution (dashed line). The peak of the distribution is at $E_g \sim 3.13$ eV, with a variance of 0.10 eV. These data suggest an average In content of $x \sim 0.15$ and a fluctuation $\Delta x = \pm 0.04$ in excellent agreement with the result of the strain analysis.

In conclusion, we find that the indium distribution inside a high-brightness GaN/InGaN green-light LED is not homogeneous. Instead, indium is enriched in clusters of 1-3 nm size and depleted around them. This inhomogeneity can be quantified by local strain measurements and by local variations of the InGaN band gap that we demonstrate here for the first time. It has been argued that a miscibility gap in the InN-GaN system favours the indium segregation. Consequently, details of the segregation process must critically depend on the growth process. It was suggested before that the growth procedure is essential for the performance of such a device[1,6,15]. Our results are consistent with a model that describes local band gap minima as dominant, local recombination centres[16], thereby suppressing non-radiative recombination at dislocations that are present in high density ($2\text{-}10\times10^{10}$ cm^{-2}) in these devices[27].

Methods

SAMPLE PREPARATION

Commercially available InGaN/GaN green-light LEDs grown by low-pressure metal-organic chemical vapour deposition are investigated. Samples were prepared site-specific from the active device area utilizing a focused ion beam (FIB) process. A sub sequential wet etching procedure with a 25% KOH aqueous solution[19] was applied that removes the sidewall damage provoked by the bombardment of the specimen with heavy Ga^{2+} ions (details in ref. 12).

ELECTRON MICROSCOPY AND IMAGE ANALYSES

Z-contrast images were recorded in two microscopes. Medium resolution Annular-Dark-Field TEM images were obtained with a CM300 FEG/UT transmission electron microscope operating at 150kV[14]. This method used an annular dark field aperture in the back focal plane of the objective lens to produce a Z-contrast image. Atomic resolution Z-contrast imaging (or high-angle annular dark-field scanning transmission electron microscopy, HAADF-STEM) was performed using a monochromated FEI Tecnai F20 UT microscope that operates at 200keV and allows for focusing of the electron beam to a 0.14 nm wide spot. The attached monochromator enables reducing the energy spread of the zero-loss peak to values below 200 meV[28,29], which is essential for the recording of low loss spectra (VEELS).

High-resolution lattice images were recorded with the Berkeley Atomic Resolution Microscope (ARM) operated at 800keV. Utilization of high electron energy allows penetrating samples of thickness t that is much larger than the quantum well width w ($t >$

10w). Therefore, thin-foil relaxation in the TEM samples can neglected, which is crucial for a reproducible extraction of local displacements.

Intensity maxima in lattice images were determined by fitting of model functions that pinpoint the position of intensity maxima to a precision of 0.1 pixel (2 pm). The resulting positions relate to the crystal structure and can be used to locally measure the size of each unit cell. This information is converted to produce maps of local displacements[30].

Acknowledgements

This research was supported by the Laboratory Technology Research Division (SC-32), within the Office of Science, US Department of Energy under a CRADA (Contract DE-AC03-76SF00098). The authors acknowledge support of the staff and the facilities at NCEM. J.R.J. wishes to thank the Alexander-von-Humboldt Foundation, Bonn/Germany. One of the authors (R.E.) was supported by the US Department of Energy under grant number DE-FG02-03ER46057.

Competing financial interests

The authors declare that they have no competing financial interests.

References

1. Nakamura, S. The Roles of Structural Imperfections in InGaN-Based Blue Light–Emitting Diodes and Laser Diodes. *Science* **281**, 956-961 (1998).
2. Ponce, F. A. & Bour, D. P. Nitride-based semiconductors for blue and green light-emitting devices. *Nature* **386**, 351-359 (1997).
3. Okamoto, K. et al. Surface-plasmon-enhanced light emitters based on InGaN quantum wells. *Nature Materials* **3**, 601-605 (2004).
4. Gardner, N. F., Craford M. G. & Steranka F. M. Diodes, light-emitting. in *Optics Encyclopedia* **1**, 275-325, Brown T. G. et al., eds. (Wiley-VCH Verlag, Weinheim, Germany, 2004).
5. Krames, M.R. et al. High-power truncated-inverted-pyramid $(Al_xGa_{1-x})_{0.5}In_{0.5}P/GaP$ light-emitting diodes exhibiting >50% external quantum efficiency. *Appl. Phys. Lett.* **75**, 2365-2367 (1999).
6. O'Donnell, K. P., Martin, R. W. & Middleton, P. G. Origin of Luminescence from InGaN Diodes. *Phys. Rev. Lett.* **82**, 237-240 (1999).
7. O'Donnell, K. P. A Mystery Wrapped in an Enigma: Optical Properties of InGaN Alloys. *phys. stat. sol. (a)* **183**, 117-120 (2001).
8. Ho, I. & Stringfellow, G. B. Solid phase immiscibility in GaInN. *Appl. Phys. Lett.* **69**, 2701-2703 (1996).
9. Watanabe, K. et al, Atomic-scale strain field and In atom distribution in multiple quantum wells InGaN/GaN. *Appl. Phys. Lett.* **82**, 715-717 (2003).
10. Takeguchi, M., McCartney, M.R. & Smith, D. J. Mapping In concentration, strain, and internal electric field in InGaN/GaN quantum well structure. *Appl. Phys. Lett.* **84**, 2103-2105 (2004).

11. O'Neill, J.P., Ross, I.M., Cullis, A.G., Wang, T. & Parbrook, P. J. Electron-beam-induced segregation in InGaN/GaN multiple-quantum wells. *Appl. Phys. Lett.* **83**, 1965-1967 (2003).
12. Jinschek, J.R., Radmilovic, V. & Kisielowski, C. FIB Preparation for HRTEM: GaN Based Devices. *Microsc. Microanal.* **10** (Suppl.2), 1142-1143 (2004).
13. Browning, N. D., Chisholm, M. F., Pennycook, S. J. Atomic-resolution chemical analysis using a scanning transmission electron microscope, *Nature* **366**, 143-146 (1993).
14. Bals, S., Kabius, B., Haider, M., Radmilovic, V. & Kisielowski, C. Annular dark field imaging in a TEM. *Solid State Communications* **130**, 675-680 (2004).
15. Narukawa, Y. et al. Role of self-formed InGaN quantum dots for exciton localization in the purple laser diode emitting at 420 nm. *Appl. Phys. Lett.* **70**, 981-983 (1997).
16. Mukai, T., Yamada, M. & Nakamura, S. Current and Temperature Dependences of Electroluminescence of InGaN-Based UV/Blue/Green Light-Emitting Diodes. *Jpn. J. Appl. Phys.* **37**, L1358-L1361 (1998).
17. Lakner, H. et al. Investigation of inhomogeneities in (Al, Ga, In)N heterostructures by STEM and cathodoluminscence. *Materials Science & Engineering B* 51, 44-52 (1998).
18. Kisielowski, C. Composition and Strain Fluctuations in InN/GaN/AlN Heterostructures: A Microscopic Glimpse below Surfaces. *Proceedings of the 2nd International Symposium on Blue Laser and Light Emitting Diodes* (Ohmsha Ltd., Tokyo), 321-326 (1998).

19. Kisielowski, C., Lilienthal-Weber Z. & Nakamura, S. Atomic Scale Indium Distribution in a GaN/$In_{0.43}Ga_{0.57}N/Al_{0.1}Ga_{0.9}N$ Quantum Well Structure. *Jpn. J. Appl. Phys.* **36**, 69-32-6936 (1997).
20. Batson, P. E., Kavanagh, K. L., Woodall, J. M. & Mayer, J. W. Electron-Energy-Loss Scattering near a Single Misfit Dislocation at the GaAs/GaInAs Interface. *Phys. Rev. Lett.* **57**, 2729-2732 (1986).
21. Rafferty, B. & Brown, L. M. Direct and indirect transitions in the region of the band gap using electron-energy-loss spectroscopy. *Phys. Rev. B* **58** (16), 10326-10337 (1998).
22. Egerton, R.F. New techniques in electron energy-loss spectroscopy and energy-filtered imaging. *Micron* **34**, 127-139 (2003).
23. Keast, V. J., Scott, A. J., Kappers, M. J., Foxon, C. T. & Humphreys, C. J. Electronic structure of GaN and $In_xGa_{1-x}N$ measured with electron energy-loss spectroscopy. *Phys. Rev. B* **66**, 125319(1-7) (2002).
24. Brockt, G. & Lakner, H. Nanoscale EELS analysis of dielectric function and bandgap properties in GaN and related materials. *Micron* **31**, 435-440 (2002).
25. Logothetidis, S., Petalas, J., Cardona, M. & Moustakas, T.D. Optical properties and temperature dependence of the interband transitions of cubic and hexagonal GaN. *Phys. Rev. B* **50**, 18017-18029 (1994).
26. Wright, A. F. & Nelson, J. S. Bowing parameter for zinc-blende $Al_{1-x}Ga_xN$ and $Ga_{1-x}In_xN$. *Appl. Phys. Lett.* **66**, 3051-3053 (1995).

27. Lester, S.D., Ponce, F.A., Craford, M.G. & Steigerwald, D.A. High dislocation densities in high efficiency GaN-based light-emitting diodes. *Appl. Phys. Lett.* **66**, 1249-1251 (1995).
28. Tiemeijer, P.C. Measurement of Coulomb interactions in an electron beam monochromator. *Ultramicroscopy* **78**, 53-62 (1999).
29. Brink, H. A., Barfels, M. M. G., Burgner, R. P. & Edwards, B. N. A sub-50 meV spectrometer and energy filter for use in combination with 200 kV monochromated (S)TEMs. *Ultramicroscopy* **96**, 367-384 (2003).
30. Schwander, P. et al. Mapping Projected Potentials, Interfacial Roughness, and Composition in General Crystalline Solids by Quantitative Transmission Electron Microscopy. *Phys. Rev. Lett.* **71**, 4150-4153 (1993)

Figure legends:

Figure 1

Annular dark-field (scanning) transmission electron micrographs of InGaN quantum wells in the active LED region;

(a) ADF-TEM image

(b) Z-contrast micrographs (HAADF-STEM), (left) in grey scale and (right) in false colour code.

Figure 2

(a) HRTEM lattice image of an InGaN quantum well. Areas (indicated by arrows) show local large expansion of the lattice inside the quantum well (defects);

(b) Strain analysis: average strain measured in (a);

(c) 2D strain map - taken from (a) - indicating strain fluctuations (green-yellow) inside the quantum well and particularly large strain inside the defects (>8%, red).

Figure 3

High energy-resolution VEEL spectra;

(a) Low-loss region of a GaN matrix spectrum (solid line) and of an InGaN quantum well spectrum (open circles);

(b) Three different GaN spectra; (c) one GaN spectrum (solid line) with a power law fit (dashed line); (d), (e) two spectra taken in the InGaN quantum wells (open circles) with power law fits (dashed lines).

Figure 4

Summary of all in our experiment measured energies of the band gap inside the InGaN quantum wells (solid line), fitted with a Poisson distribution (dashed line).

Figure 1 / Joerg R. Jinschek

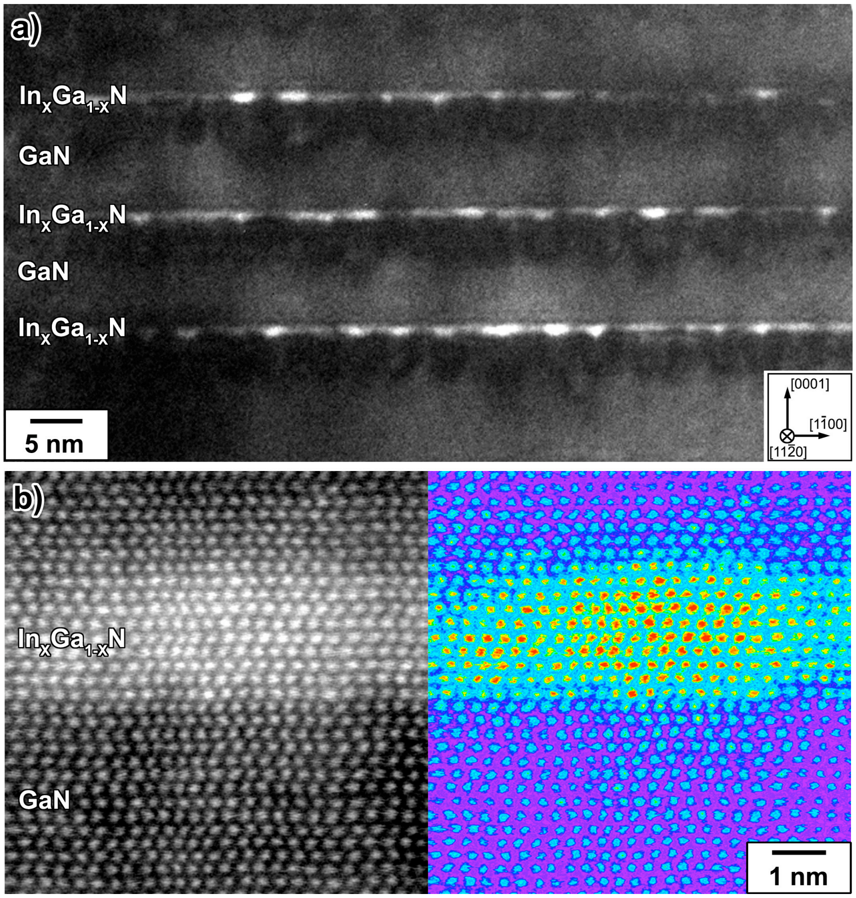

Figure 2 / Joerg R. Jinschek

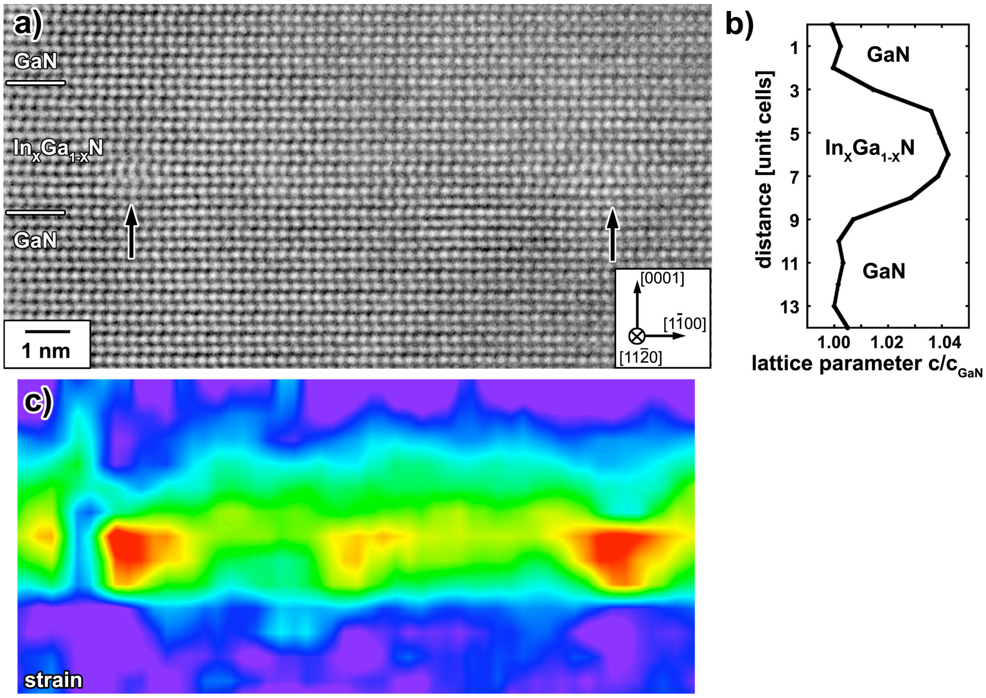

Figure 3 / Joerg R. Jinschek

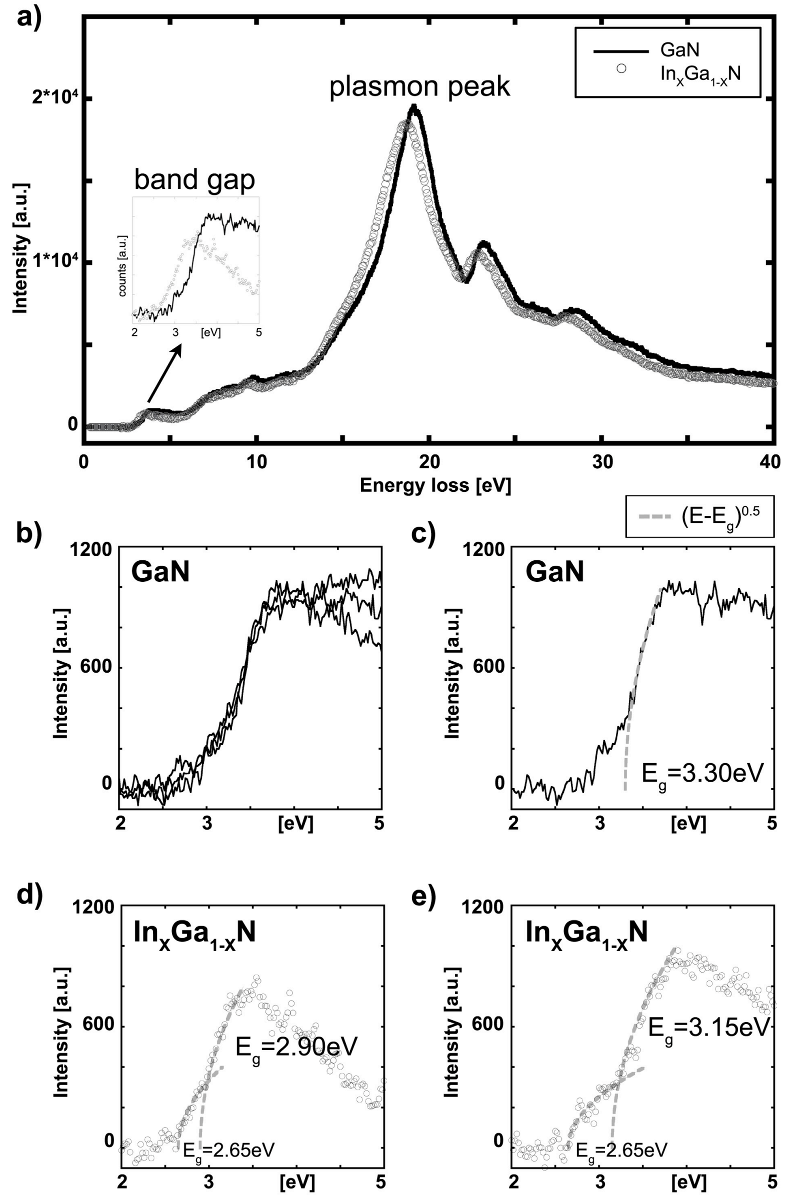

Figure 4 / Joerg R. Jinschek